INFLUENCE OF SEDIMENT RESUSPENSION ON DEEP-OCEAN ^{231}Pa & ^{230}Th: A PROGRESS REPORT

Siyuan-Sean CHEN[1,2], Olivier MARCHAL[2], Paul LERNER[3], Daniel McCORKLE[2], Michiel RUTGERS VAN DER LOEFF[4]

[1] School of Earth Sciences, University of Bristol, Bristol, UK (sc16502@bristol.ac.uk)

[2] Woods Hole Oceanographic Institution, Woods Hole, MA, USA

[3] NASA Goddard Institute for Space Studies, New York, NY, USA

[4] Alfred Wegener Institute for Polar and Marine Research, Bremerhaven, Germany

EGU General Assembly 2020

SCIENTIFIC CONTEXT

- Protactinium-231 (^{231}Pa) and thorium-230 (^{230}Th) are two naturally-occurring, particle-reactive radioisotopes that have found various applications in chemical oceanography and paleoceanography.

- Both tracers are core parameters of GEOTRACES, an ongoing international program aimed at the study of the ocean biogeochemical cycles of trace elements and isotopes.

- Analyses of deep water samples collected along GEOTRACES transect GA03 in the North Atlantic showed small ^{231}Pa and ^{230}Th activities in the dissolved phase and very large ^{231}Pa and ^{230}Th activities in the particulate phase that are difficult to rationalize based on current understanding about the cycling of both radionuclides in the ocean.

- The proximity of these ^{231}Pa and ^{230}Th anomalies to the seafloor suggests that these may have originated from the interaction with resuspended sediment.

- The overarching goal of this research is to study the influence of sediment resuspension on the vertical distributions of ^{231}Pa and ^{230}Th in the lower water column and the upper sediment column.

THE U.S. GEOTRACES NORTH ATLANTIC TRANSECT GA03 (next page)

- The U.S. GEOTRACES North Atlantic transect GA03 comprised two legs (see top figure on next page): stations occupied during leg 1 are labelled GT10-n and stations occupied during leg 2 are labelled GT11-n, where n is station number.

- The GA03 stations occupied in the western North Atlantic between the New England continental shelf and Bermuda were aligned along “line W”, an oceanographic line that has been the focus of other field programs (see bottom figure on next page).

- Two major oceanic currents cross line W: the Gulf Stream near the surface and the Deep Western Boundary Current at depth. The first of these currents flows to the northeast and the second flows to the southwest.

THE U.S. GEOTRACES NORTH ATLANTIC TRANSECT GA03

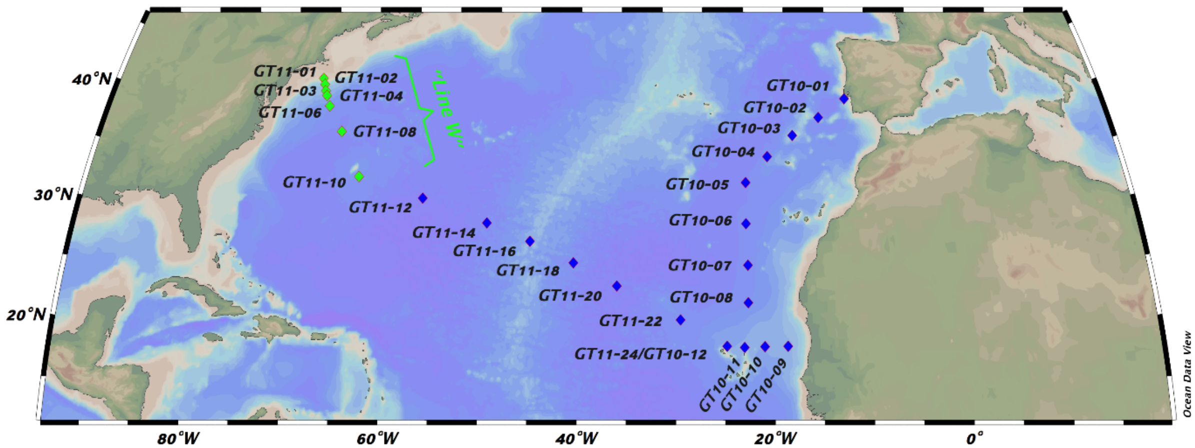

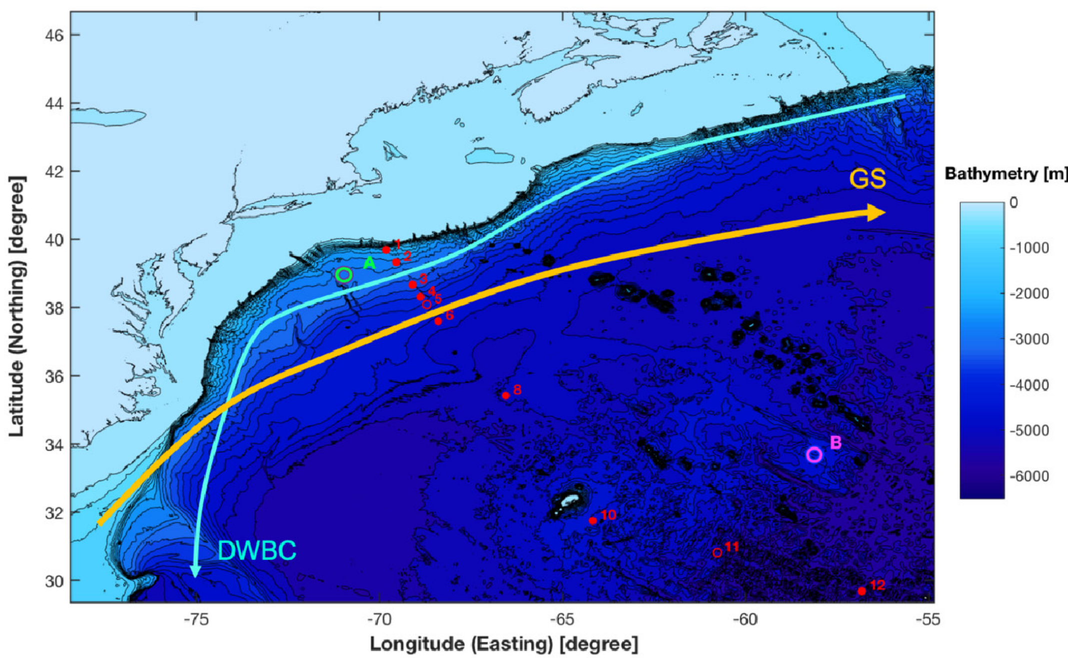

GA03 stations

Gulf Stream

Deep Western Boundary Current

A,B surface sediment samples

HYDROGRAPHIC PROFILES IN WESTERN NORTH ATLANTIC (next page)

- Measurements of potential temperature and salinity indicate that a bottom mixed layer with a thickness of O(100 m) was present at GA03 stations visited along line W (potential temperature is the temperature a water parcel would have if it were brought adiabatically to the sea surface).

- Concomitant measurements of particulate matter (PM) concentration estimated from beam transmissometry (light attenuation) show that PM concentration generally increased with depth in the lower kilometer of the water column. Maxima in PM concentration were observed in the bottom mixed layers.

- This region of increased PM concentration with depth is called the Benthic Nepheloid Layer (BNL). In the western North Atlantic, the BNL extends from the bottom up to a depth of typically 3000 m. In general, BNLs are thought to originate from the resuspension of seafloor sediment.

HYDROGRAPHIC PROFILES IN WESTERN NORTH ATLANTIC

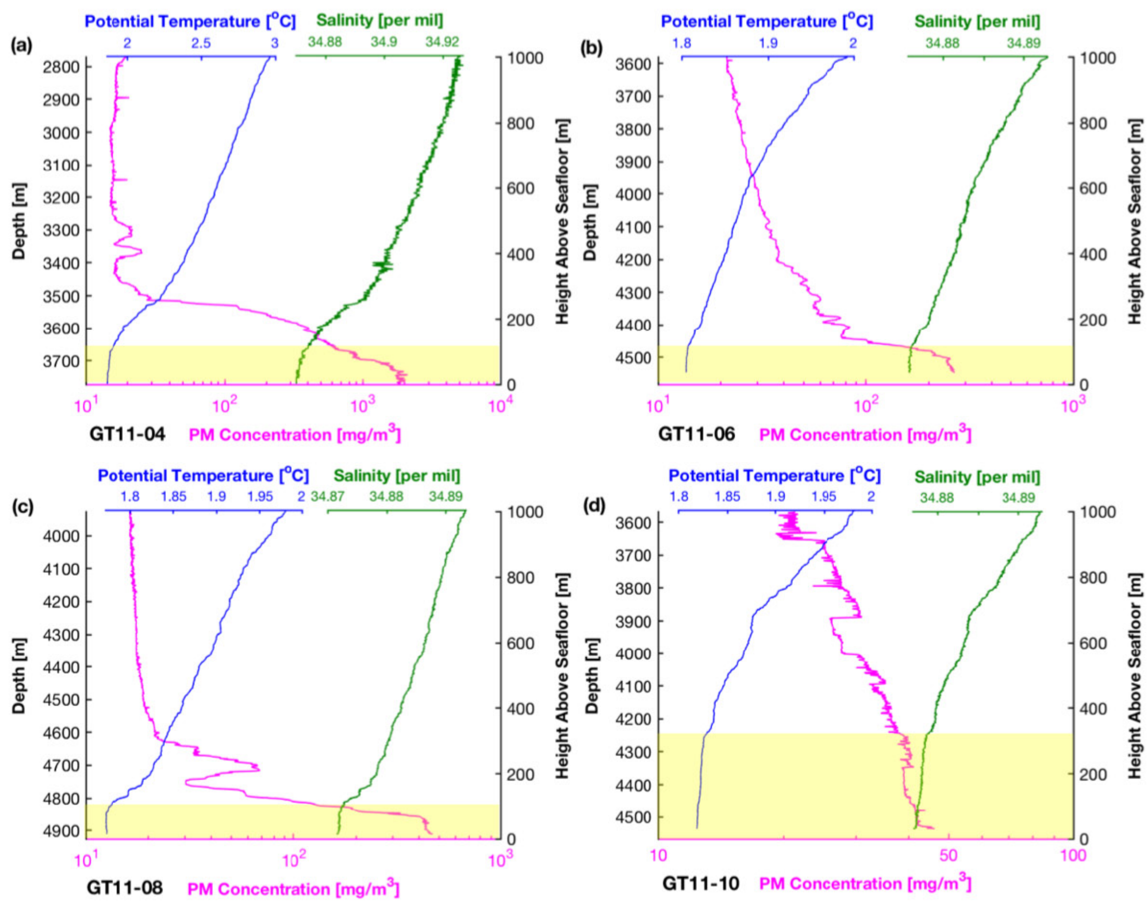

PM Particulate Matter

Bottom Mixed Layer

data from *Schlitzer et al*. (2018)

POTENTIAL TEMPERATURE – SALINITY DIAGRAM FOR DEEP (> 3000 m) WATERS (next page)

- The potential temperature – salinity diagram for deep waters at GA03 stations along line W shows that these waters could be described as variable mixtures of three major deep water masses in the North Atlantic: Denmark Strait Overflow Water (DSOW), Iceland-Scotland Overflow Water (ISOW), and Classical Labrador Sea Water (CLSW).

- Measurements of the dissolved silica concentration of the deep waters (not shown) suggest that these waters could also contain a significant proportion of the silicate-rich Antarctic Bottom Water (AABW) that originates from the Southern Ocean.

POTENTIAL TEMPERATURE – SALINITY DIAGRAM FOR DEEP (> 3000 m) WATERS

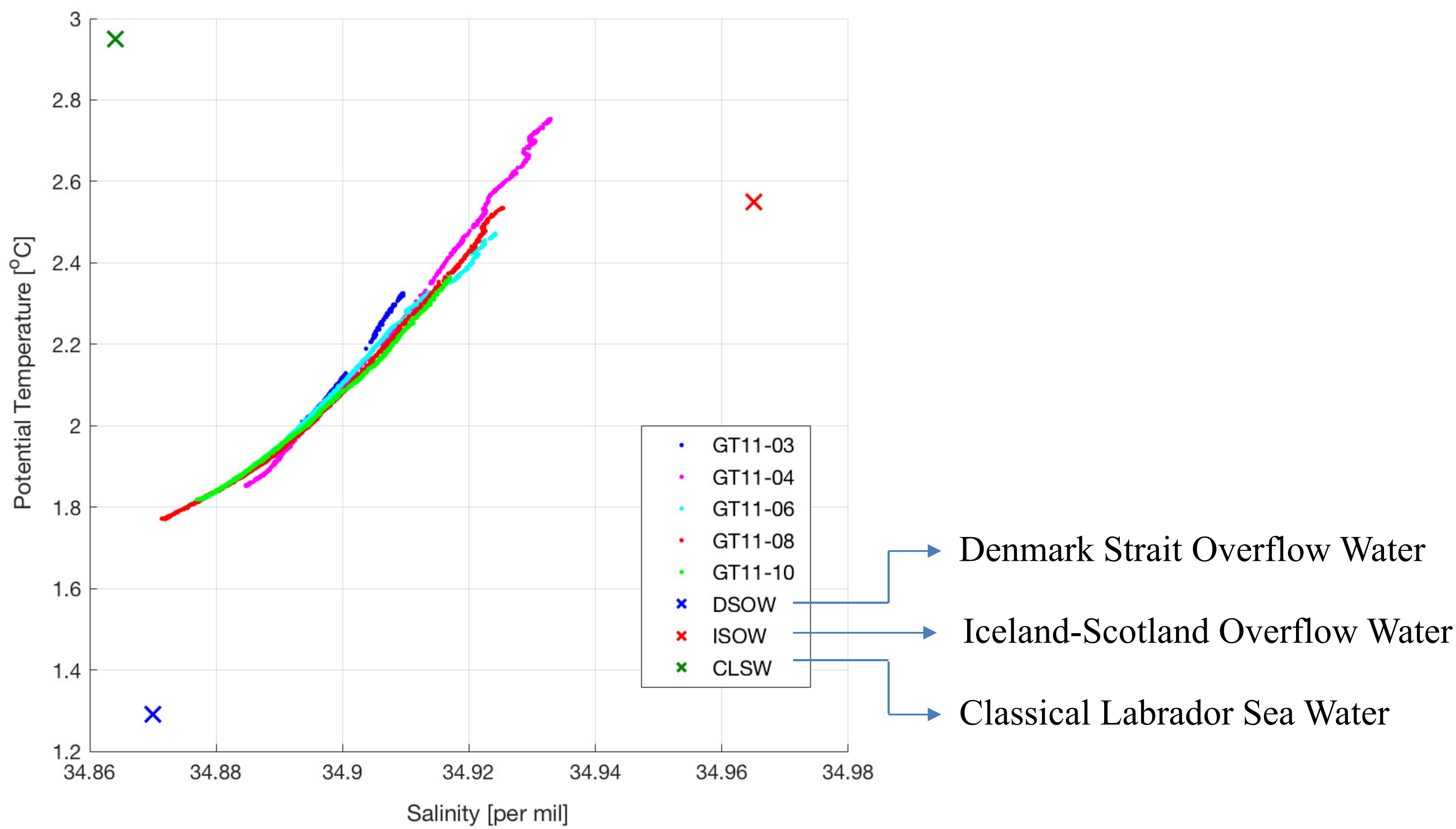

data from *Schlitzer et al*. (2018)

PROFILES OF PARTICLE CONCENTRATION & RADIONUCLIDE ACTIVITIES (next 2 pages)

- Analyses of deep water samples collected at GA03 stations along line W showed small ^{231}Pa and ^{230}Th activities in the dissolved phase and very large ^{231}Pa and ^{230}Th activities in the particulate phase in deep waters.

- These activity anomalies are difficult to reconcile with a popular model that describes the vertical distributions of ^{231}Pa and ^{230}Th in the ocean (Bacon and Anderson 1982). In this model, the dissolved activities increase with depth throughout the water column and the particulate activities do not reach values as high as those observed.

- The fact that the observed ^{231}Pa and ^{230}Th anomalies tend to be found in BNLs suggests that sediment resuspension, a process not included in the model mentioned above, could have been at least partly responsible.

PROFILES OF PARTICLE CONCENTRATION & RADIONUCLIDE ACTIVITIES

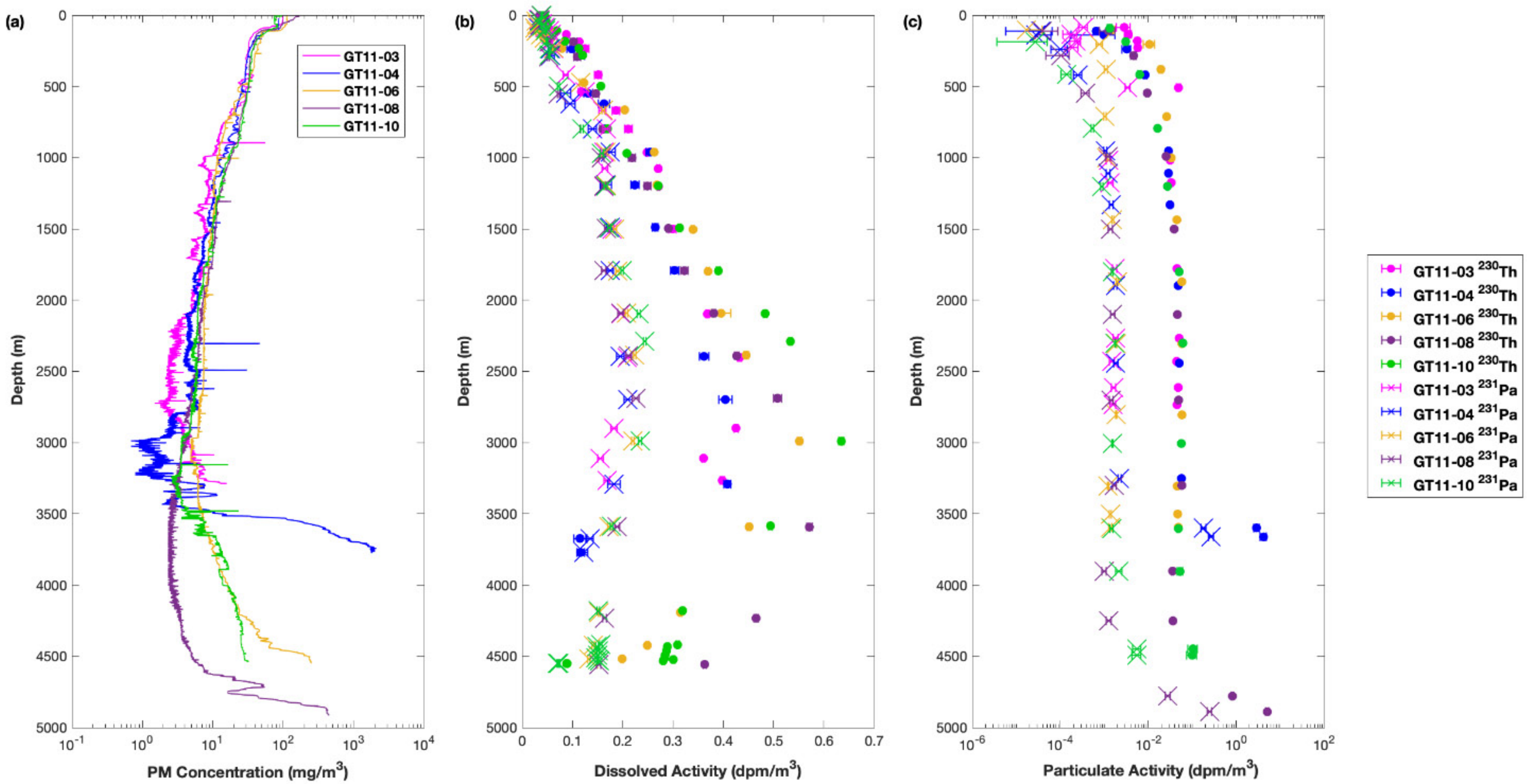

data from *Schlitzer et al*. (2018)

PROFILES OF PARTICLE CONCENTRATION & RADIONUCLIDE ACTIVITIES

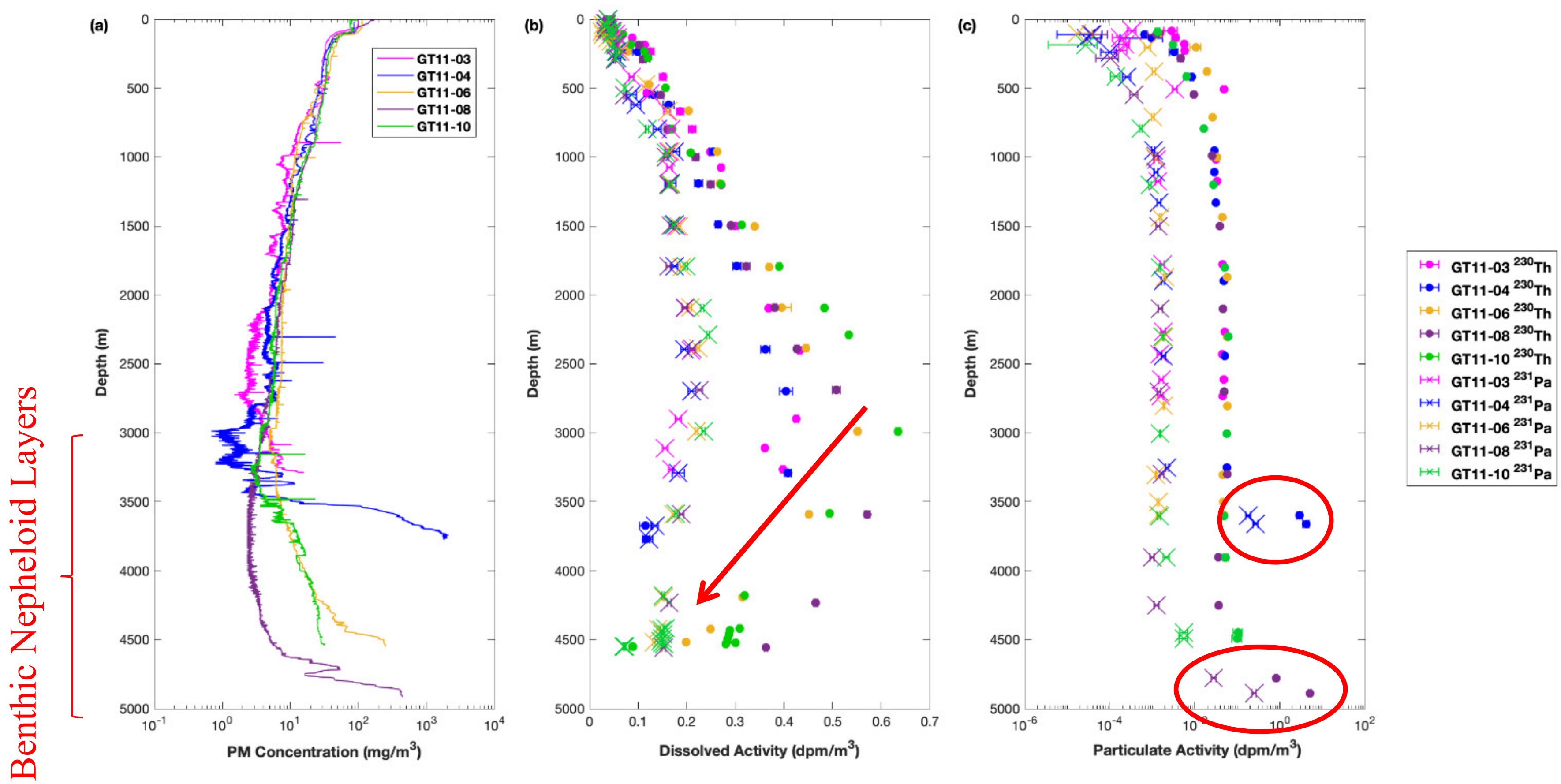

data from *Schlitzer et al*. (2018)

RESEARCH QUESTION

What is the influence of sediment resuspension on the vertical distributions of ^{231}Pa & ^{230}Th in the lower water column and upper sediment?

RESEARCH APPROACH

- Develop a 1D (vertical) model of particle, ^{231}Pa, and ^{230}Th cycling in the BNL & the sediment. This model relies on, and extends, the models of Boudreau (1997a) and of Rutgers van der Loeff and Boudreau (1997).

- Compare model results with *in situ* measurements (water & sediment).

- Apply the model in sensitivity experiments.

SCHEMATIC OF THE MODEL OF PARTICLE, ^{231}Pa, AND ^{230}Th CYCLING

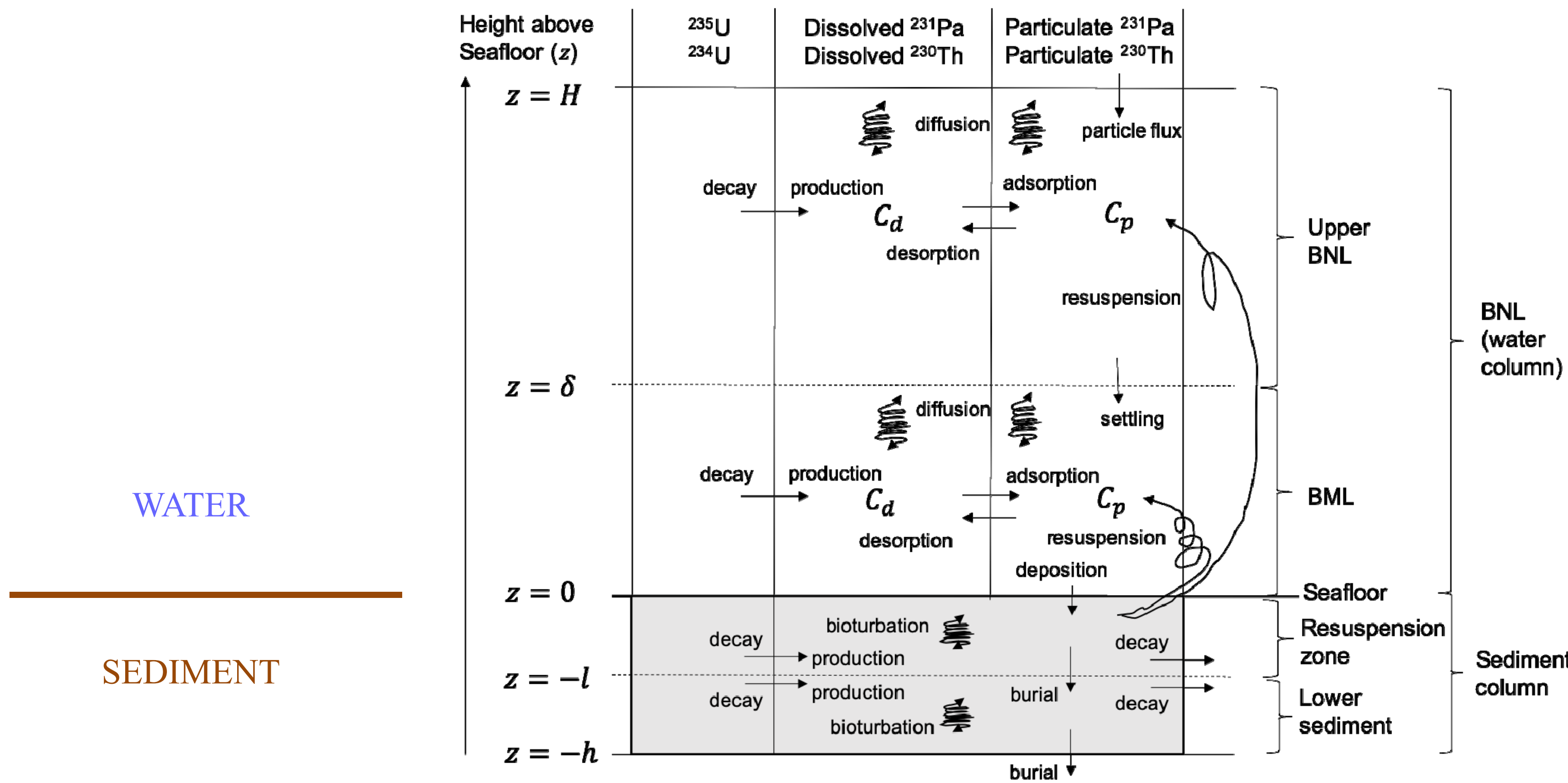

TREATMENT OF RESUSPENSION AS A NON-LOCAL PROCESS

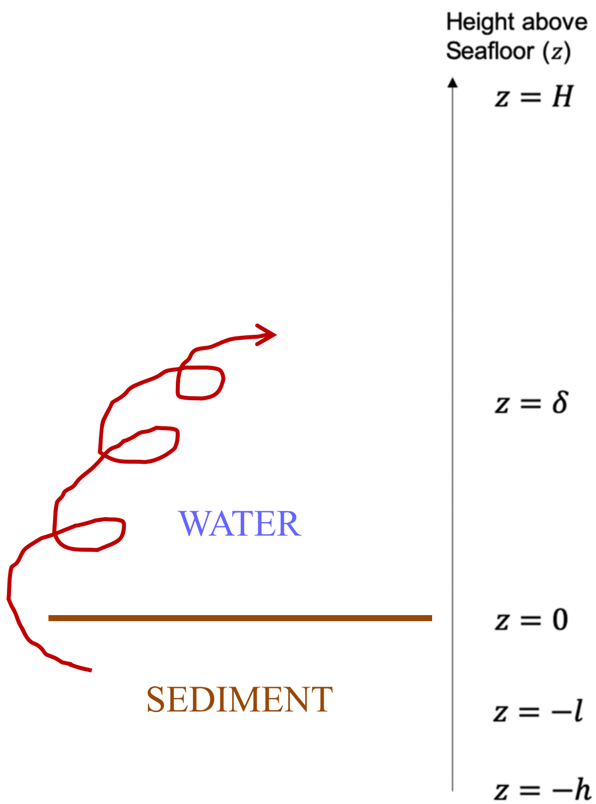

sediment injection rate = $\dot{\varphi}_r e^{-z/\delta_r}$

with

$$\int_0^H \underbrace{\dot{\varphi}_r}_{\text{injection rate at } z=0} e^{-z/\overbrace{\delta_r}^{\text{injection height scale}}} dz = \int_{-l}^{0} \underbrace{K}_{\text{resuspension rate}} \overbrace{\varphi_s}^{\text{solid volume fraction}} dz$$

Boudreau (1997a)

MODEL OF PARTICLE & RADIONUCLIDE CYCLING

- The next pages describe in mathematical terms the model of particle and radionuclide cycling that has been developed.

- This model assumes steady state (the unsteadiness term $\partial/\partial t$ is omitted from the governing equations) and neglects all transport processes except vertical turbulent mixing (the effects of horizontal and vertical advection, and the effects of horizontal mixing are omitted).

- In this model, sediment resuspension is treated as a non-local process, i.e., it is represented as a source term in the governing equations for particles and for the particulate phase, and not in the boundary conditions of the differential equations for these variables.

MODEL OF PARTICLE CYCLING

- Governing Equation

$$\frac{\partial \varphi}{\partial t} + \frac{\partial}{\partial z}\Bigg(\underbrace{w_p \varphi}_{\textit{settling}} - \underbrace{E\frac{\partial \varphi}{\partial z}}_{\textit{mixing}}\Bigg) = \underbrace{\dot{\varphi}_r e^{-z/\delta_r}}_{\textit{resuspension}}$$

- Boundary Conditions

$$w_p \varphi - E\frac{\partial \varphi}{\partial z} = \frac{F_p}{\rho_p} \qquad \text{at } z = H$$

$$-E\frac{\partial \varphi}{\partial z} = 0 \qquad \text{at } z = 0$$

Boudreau (1997a)

PARAMETERS OF PARTICLE CYCLING MODEL

Symbol	Definition	Reference Value	Units	Reference
w_p	particle settling speed	-5.8	m/d	Gardner et al. (1985)
E_1	diffusivity in lower BNL	5×10^{-3}	m^2/s	Sarmiento & Biscaye (1986)
E_2	diffusivity in upper BNL	5×10^{-4}	m^2/s	Sarmiento & Biscaye (1986)
K	sediment erosion rate	variable*	1/d	Boudreau (1997a)
l	erosion zone thickness	0.01	m	Boudreau (1997a)
δ_r	resuspension height scale	variable*	m	Boudreau (1997a)
φ_s	sediment volume fraction	0.1	unitless	Boudreau (1997a)

* Parameter varied in sensitivity experiments

PARTICLE CONCENTRATION PROFILE: Effect of Sediment Erosion Rate ($\delta_r = 1$ m)

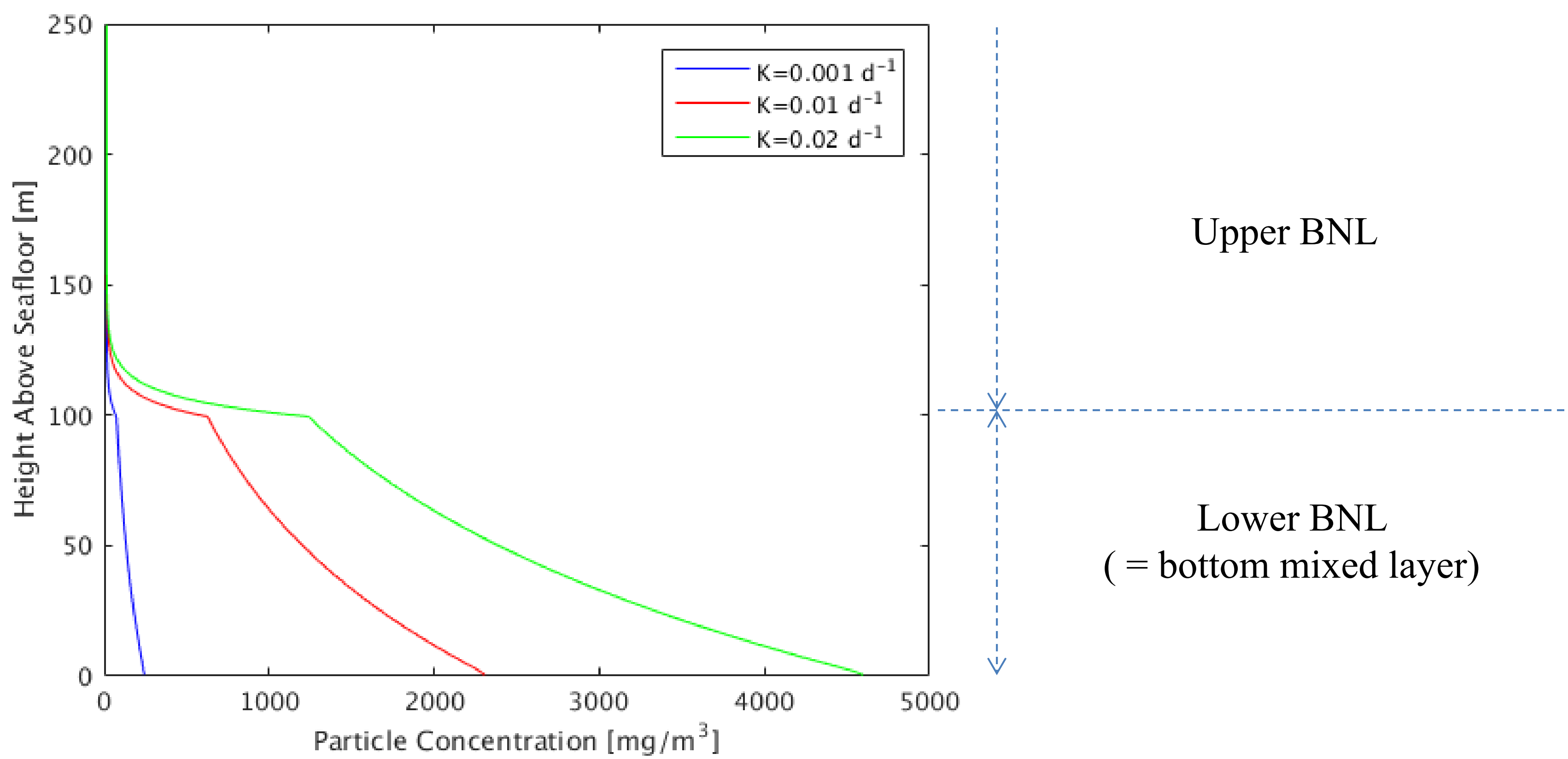

PARTICLE CONCENTRATION PROFILE: Effect of Resuspension Height Scale ($K = 0.01$ d^{-1})

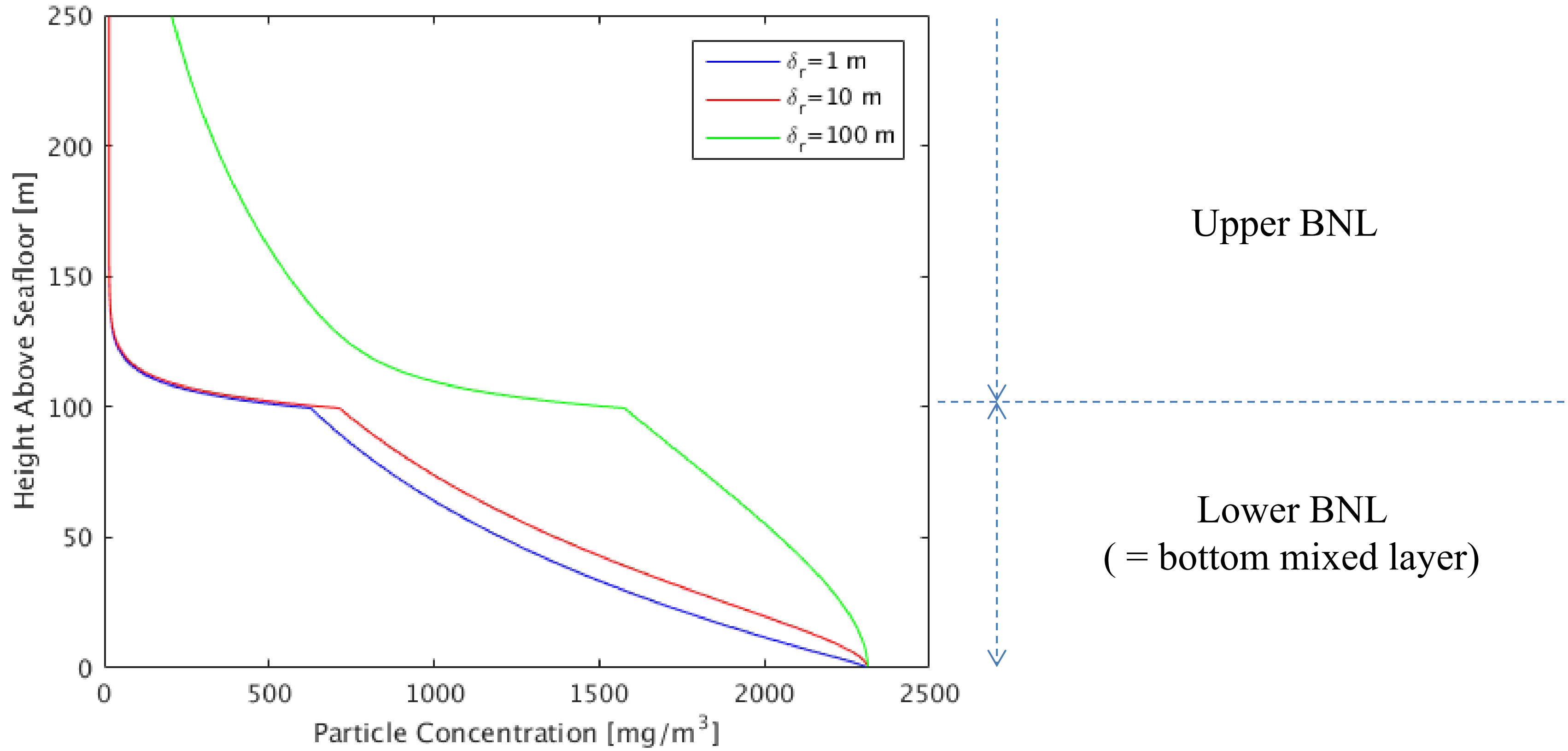

MODEL OF ^{231}Pa & ^{230}Th CYCLING: Water Column

- Governing Equations

dissolved phase: $$\frac{\partial C_d}{\partial t} + \frac{\partial}{\partial z}\underbrace{\left(-E\frac{\partial C_d}{\partial z}\right)}_{\textit{mixing}} = \overbrace{\beta}^{\textit{production}} + \underbrace{k_{-1}C_p}_{\textit{desorption}} - \overbrace{k_1 C_d}^{\textit{adsorption}}$$

particulate phase: $$\frac{\partial C_p}{\partial t} + \frac{\partial}{\partial z}\left(\underbrace{w_p C_p}_{\textit{settling}} - \underbrace{E\frac{\partial C_p}{\partial z}}_{\textit{mixing}}\right) = \overbrace{k_1 C_d}^{\textit{adsorption}} - \underbrace{k_{-1}C_p}_{\textit{desorption}} + \overbrace{\dot{\varphi}_r B_r e^{-z/\delta_r}}^{\textit{resuspension}}$$

- Boundary Conditions

$$C_d = C_{d,H} \qquad C_p = C_{p,H} \qquad \text{at } z = H$$

$$-E\frac{\partial C_d}{\partial z} = 0 \qquad w_p C_p = w_s \varphi_s B_s \qquad \text{at } z = 0$$

EFFECT OF PARTICLE CONCENTRATION ON METAL SCAVENGING

$$\overbrace{k_1(\mathrm{Me})}^{\textit{adsorption rate constant}} = \underbrace{k_1'(\mathrm{Me})}_{\textit{adsorption rate coefficient}}\overbrace{\varphi\rho_p}^{\textit{particle concentration}}$$

where

Me = Th or Pa
φ = solid volume fraction
ρ_p = particle density

Honeyman et al (1988)
Lerner et al. (2017)

MODEL OF ^{231}Pa & ^{230}Th CYCLING: Sediment Column

- Governing Equations for Dissolved & Particulate Activities

dissolved activity: $$\frac{\partial C_d}{\partial t} + \frac{\partial}{\partial z}\left(\underbrace{-[D_B + D_M]\frac{\partial C_d}{\partial z}}_{diffusion}\right) = \overbrace{\varphi_0 \beta}^{production} - \underbrace{j_C}_{exchange} - \overbrace{\lambda C_d}^{decay}$$

particulate activity: $$\frac{\partial \varphi_s B_s}{\partial t} + \frac{\partial}{\partial z}\left(\overbrace{w_s \varphi_s B_s}^{burial} - \underbrace{D_B \frac{\partial \varphi_s B_s}{\partial z}}_{diffusion}\right) = \overbrace{j_C}^{exchange} - \underbrace{\lambda \varphi_s B_s}_{decay} - \overbrace{K \varphi_s B_s}^{resuspension}$$

where

D_B: biological diffusivity (bioturbation)
D_M: molecular diffusivity

MODEL OF ^{231}Pa & ^{230}Th CYCLING: Sediment Column (cont'd)

- Governing Equation for Total Activity

$$\left(\frac{\varphi_o}{K_d}+\varphi_s\right)\frac{\partial B_s}{\partial t}+\frac{\partial}{\partial z}\left(\overbrace{w_s\varphi_s B_s}^{burial}-\underbrace{D\frac{\partial \varphi_s B_s}{\partial z}}_{diffusion}\right)=\overbrace{\varphi_o\beta}^{production}-\underbrace{\lambda\left(\frac{\varphi_o}{K_d}+\varphi_s\right)B_s}_{decay}-\overbrace{K\varphi_s B_s}^{resuspension}$$

where

$$D=\frac{\varphi_0}{K_d}D_M+\left(\frac{\varphi_0}{K_d}+\varphi_s\right)D_B\approx\varphi_s D_B$$

- Boundary Conditions

$$w_s\varphi_s B_s=w_p C_p \qquad \text{at } z=0$$

$$-D\frac{\partial \varphi_s B_s}{\partial z}=0 \qquad \text{at } z=-h$$

TREATMENT OF RESUSPENDED PARTICLE ACTIVITY (B_r)

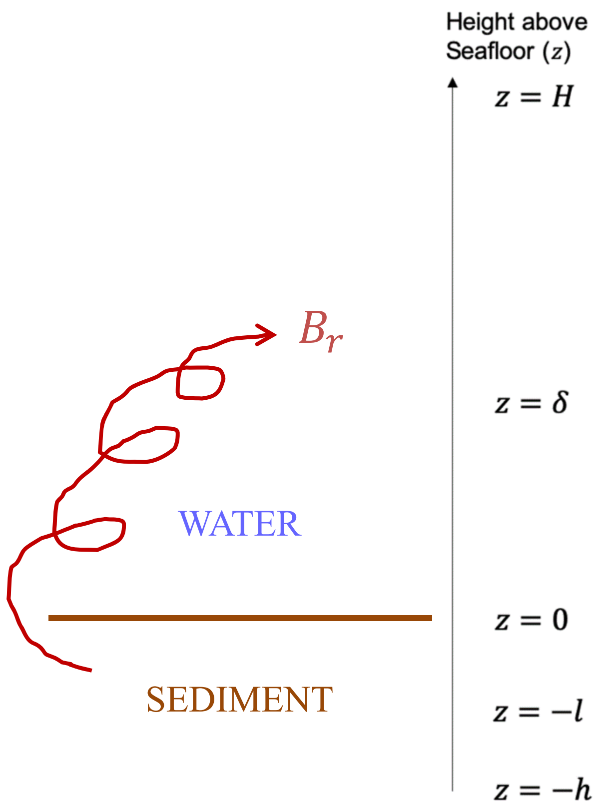

- In this presentation, B_r is fixed based on core top data
- In future work, we will consider to derive B_r from

$$\int_0^H \underbrace{\dot{\varphi}_r B_r}_{\textit{resuspended particle activity}} e^{-z/\delta_r}\, dz = \int_{-l}^{0} K \underbrace{\varphi_s B_s(z)}_{\textit{modeled sediment activity}} dz$$

PARAMETERS OF ^{231}Pa AND ^{230}Th CYCLING MODEL

Symbol	Definition	Reference Value	Units	Source
$\beta(^{231}\mathrm{Pa})$	^{231}Pa production rate	2.33×10^{-3}	dpm/(m^3 yr)	Yu et al. (1996)
$\beta(^{230}\mathrm{Th})$	^{230}Th production rate	2.52×10^{-2}	dpm/(m^3 yr)	Yu et al. (1996)
$\tau_{1/2}(^{231}\mathrm{Pa})$	half-life of ^{231}Pa	32.6	kyr	Cheng et al. (2013)
$\tau_{1/2}(^{230}\mathrm{Th})$	half-life of ^{230}Th	75.6	kyr	Jerome et al. (2020)
$K_d(^{231}\mathrm{Pa})$	distribution coefficient for ^{231}Pa	1×10^{6}	unitless	Hayes et al. (2015)
$K_d(^{230}\mathrm{Th})$	distribution coefficient for ^{231}Pa	1×10^{7}	unitless	Hayes et al. (2015)
$B_r(^{231}\mathrm{Pa})$	^{231}Pa activity of resuspended particles	0.2	dpm/g	Anderson et al. (1994)
$B_r(^{230}\mathrm{Th})$	^{230}Th activity of resuspended particles	3.5	dpm/g	Anderson et al. (1994)
$k_1'(\mathrm{Pa})$	adsorption rate coefficient for Pa	1.45×10^{-2}	mg / (m^3 yr)	tuned*
$k_1'(\mathrm{Th})$	adsorption rate coefficient for Th	1.45×10^{-3}	mg / (m^3 yr)	tuned*
k_{-1}	desorption rate constant	0	1/yr	tuned*
w_s	sediment burial rate	-2.5	cm/kyr	Keigwin & Jones (1989)
D_B	biological diffusivity	10	cm^2/yr	Boudreau (1997b)
ρ_p	particle density	1332	Kg/m^3	McCave et al. (1984)

* Parameter adjusted to reproduce approximately data for stations GT11-04 & GT11-08.

MODEL RESULTS: activity profiles (next 4 pages)

- Vertical profiles of ^{230}Th and ^{231}Pa activity in the water and sediment columns have been calculated from the model for different values of sediment erosion rate (K) and sediment resuspension height scale (δ_r).

- These profiles show that the main features in the observed distributions at stations GT11-04 and GT11-08 – the decrease of dissolved activities with depth in the lower water column and the very large particulate activities near the bottom – can both be reproduced by the model for certain values of model parameters.

- In particular, preliminary results suggest that the best fit of the model to activity measurements is obtained if the rate constant for Th and Pa desorption from particles (k_{-1}) is very small or zero (irreversible uptake).

- Preliminary model results also suggest that both sediment erosion rate and resuspension height scale can significantly influence activities in the water and the sediment, but that the latter parameter has a negligible effect on the radionuclide activities in the sediment.

^{230}Th ACTIVITY PROFILES: Effect of Sediment Erosion Rate ($\delta_r = 100$ m)

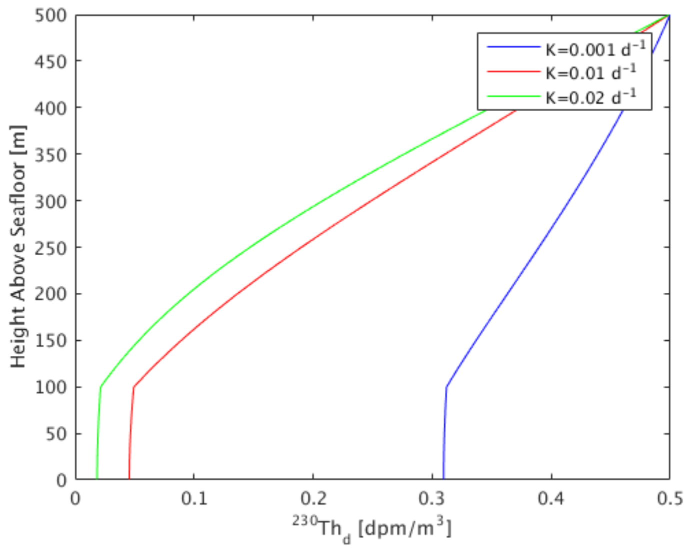

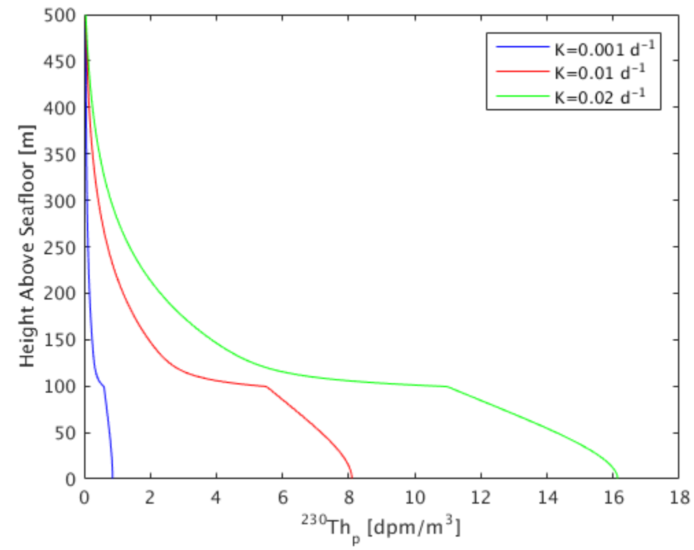

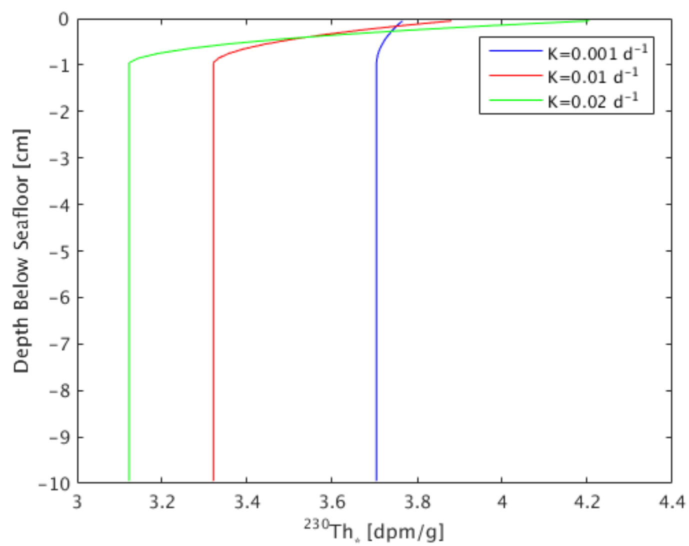

^{230}Th ACTIVITY PROFILES: Effect of Resuspension Height Scale ($K = 0.01$ d^{-1})

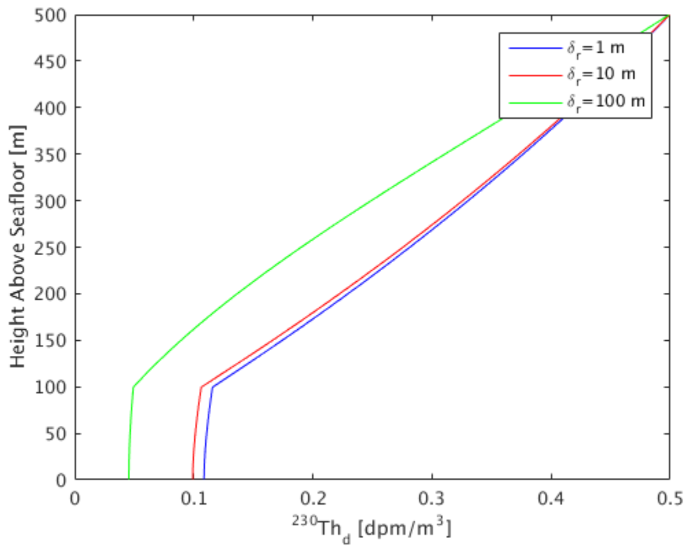

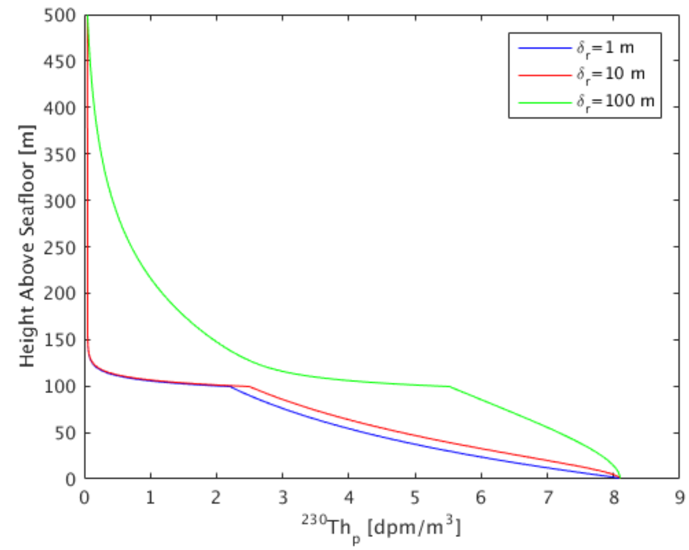

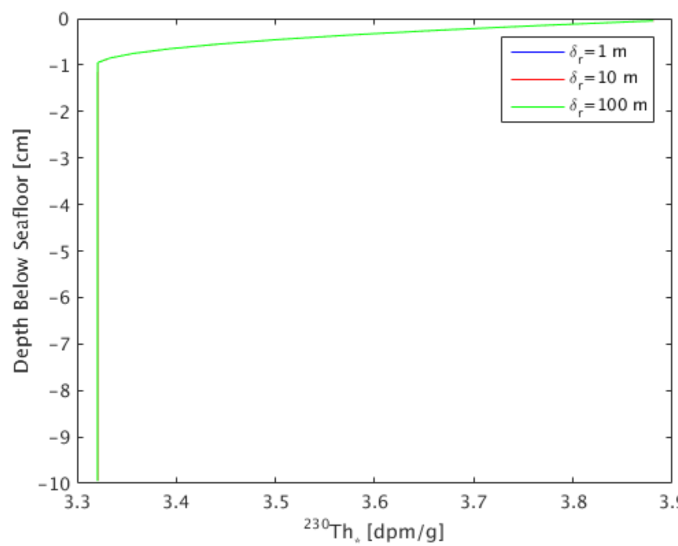

^{231}Pa ACTIVITY PROFILES: Effect of Sediment Erosion Rate ($\delta_r = 100$ m)

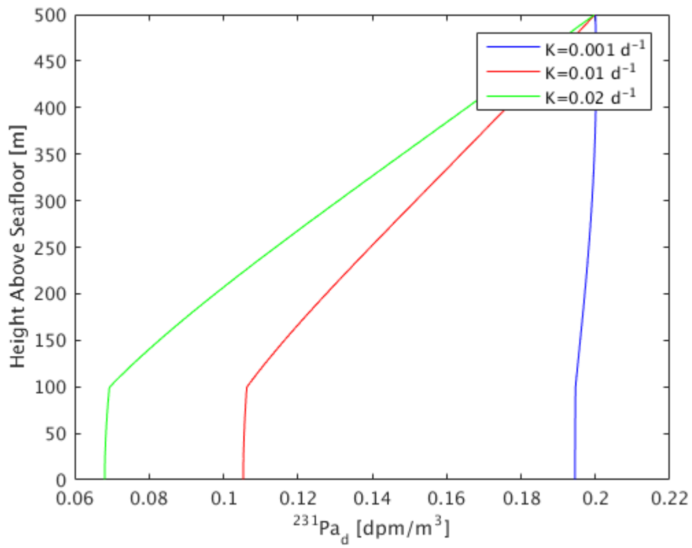

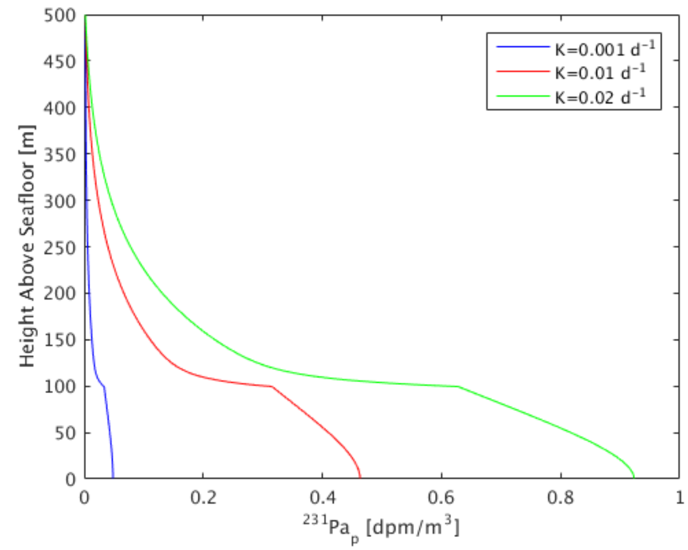

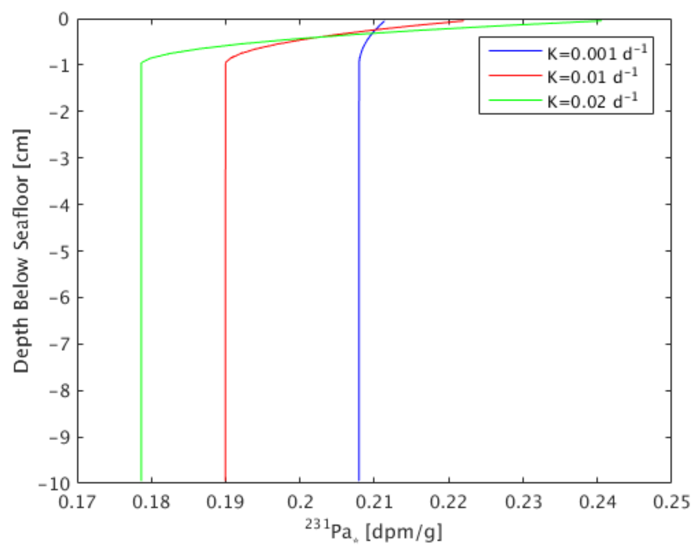

^{231}Pa ACTIVITY PROFILES: Effect of Resuspension Height Scale ($K = 0.01\ d^{-1}$)

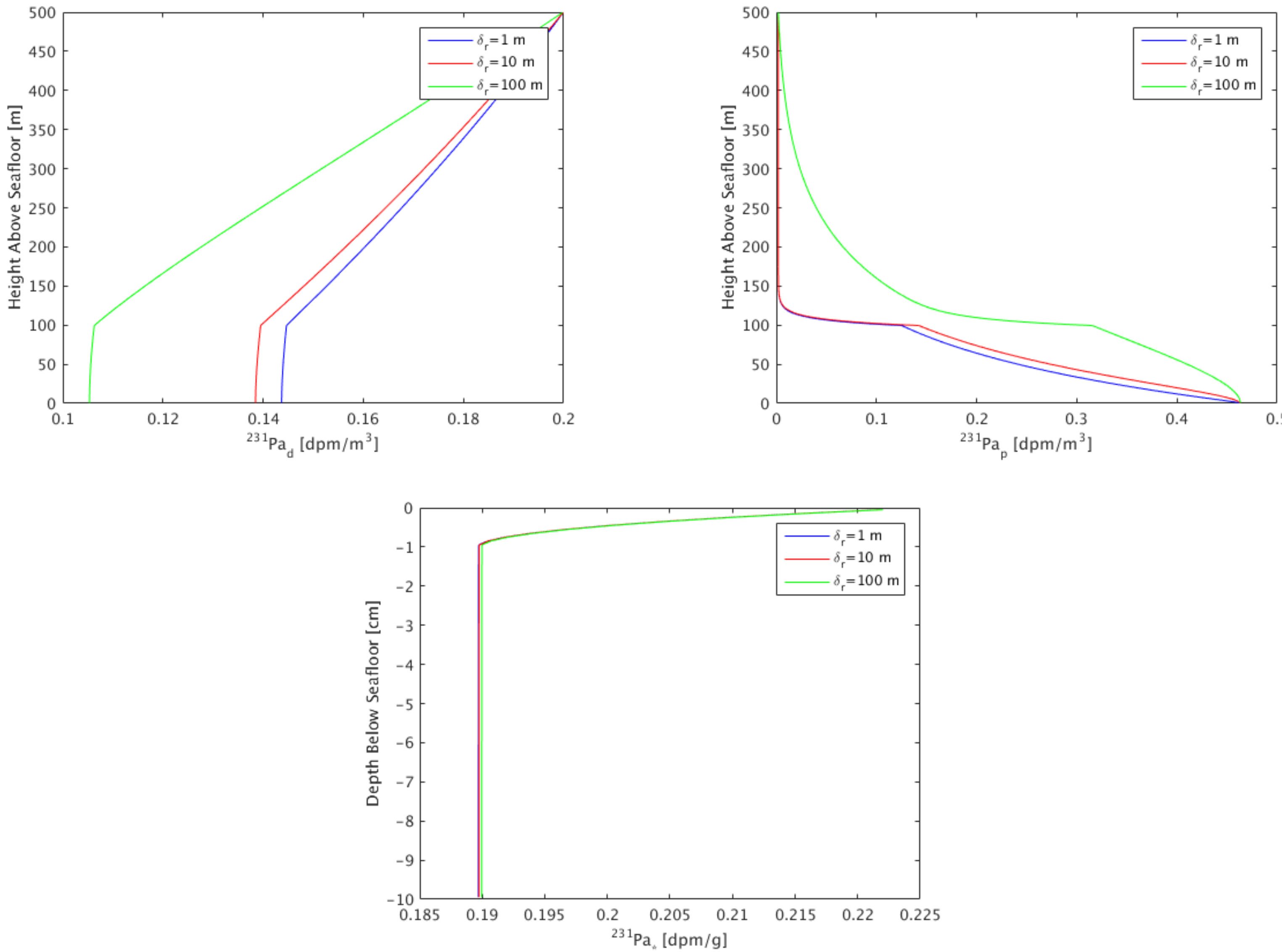

MODEL RESULTS: effect of sediment erosion rate on sediment activities (next page)

- The mean activities of ^{231}Pa and ^{230}Th in the sediment (averages from $z = -h$ to $z = 0$ m) have been calculated for different values of sediment erosion rate within a range a observational estimates.

- These preliminary calculations show that the mean sediment activity decreases with sediment erosion rate for both radionuclides: the mean sediment activity decreases from > 0.6 dpm/g to < 0.2 dpm/g for ^{231}Pa and from > 15 dpm/g to < 3 dpm/g for ^{230}Th.

- As a result, the sediment ^{231}Pa /^{230}Th ratio, often used as a paleoceanographic indicator, varies by $> 35\%$.

EFFECT OF SEDIMENT EROSION RATE ON MEAN SEDIMENT ^{231}Pa & ^{230}Th: preliminary results

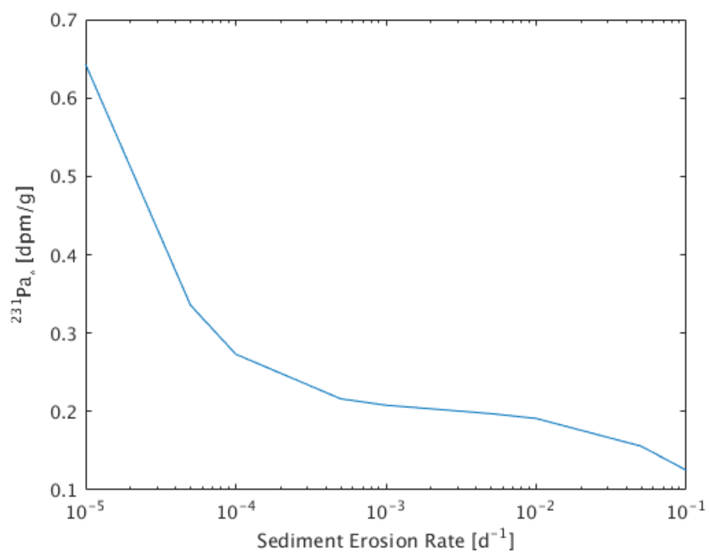

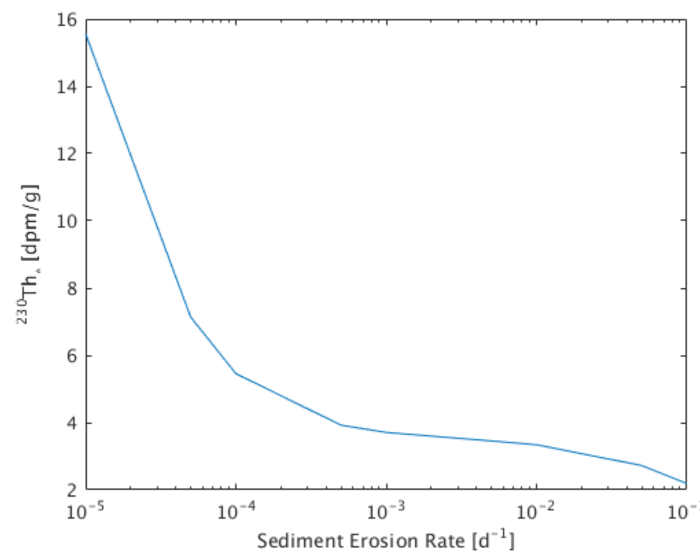

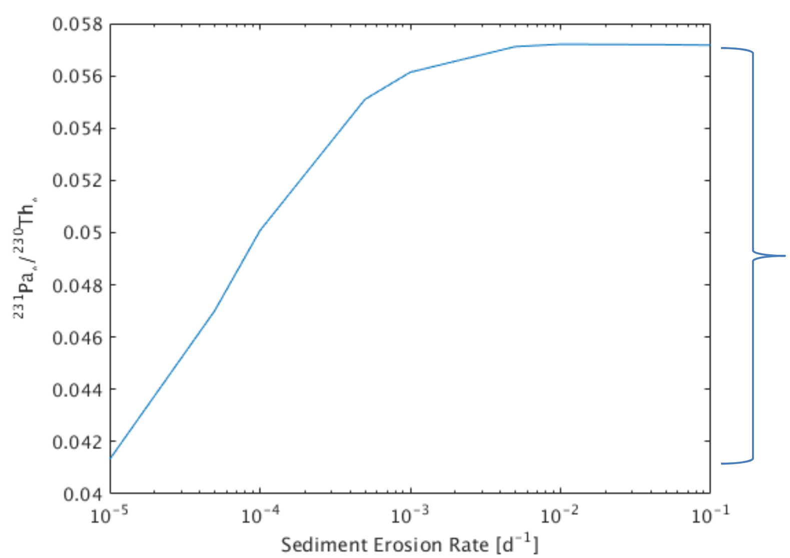

In these preliminary results, mean sediment $^{231}Pa/^{230}Th$ increases by > 35% as sediment erosion rate increases within the range of observational estimates.

CONCLUSIONS

- Benthic nepheloid layers (BNLs) were present at stations occupied along line W in the western North Atlantic during the GA03 cruise.
- The BNLs were characterized by (i) a lower region showing PM concentration maxima and coinciding with the bottom mixed layer with thickness of O(100 m), and (ii) an upper stratified region extending up to a clear water minimum at about 3000 m.
- The BNLs coincided with pronounced ^{231}Pa & ^{230}Th activity minima in the dissolved phase and very large ^{231}Pa & ^{230}Th activity maxima in the particulate phase.
- A 1D (vertical) model of particle, ^{231}Pa, ^{230}Th cycling that accounts for material exchange at the seabed was developed to examine the influence of sediment resuspension on the vertical distributions of ^{231}Pa & ^{230}Th in the lower water column and the upper sediment column.
- Preliminary results showed that the main features in PM and radionuclide profiles observed along line W can be reproduced by the model, and revealed the effects of sediment erosion rate and sediment resuspension height scale.
- Next steps: full coupling of water and sediment model components (B_r), quantitative comparison of model results to observations, application of the model to explore more comprehensively the influences of sediment resuspension.

REFERENCES

Anderson, R.F., Fleisher, M.Q., Biscaye, P.E., Kumar, N., Dittrich, B., Kubik, P. and Suter, M., 1994. Anomalous boundary scavenging in the Middle Atlantic Bight: evidence from ^{230}Th, ^{231}Pa, ^{10}Be and ^{210}Pb. *Deep Sea Research Part II: Topical Studies in Oceanography*, *41*(2-3), pp.537-561.

Bacon, M.P. and Anderson, R.F., 1982. Distribution of thorium isotopes between dissolved and particulate forms in the deep sea. *Journal of Geophysical Research: Oceans*, *87*(C3), pp.2045-2056.

Boudreau, B.P., 1997a. A one-dimensional model for bed-boundary layer particle exchange. *Journal of Marine Systems*, *11*(3-4), pp.279-303.

Boudreau, B.P., 1997b. *Diagenetic models and their implementation* (Vol. 505). Berlin: Springer.

Cheng, H., Edwards, R.L., Shen, C.C., Polyak, V.J., Asmerom, Y., Woodhead, J., Hellstrom, J., Wang, Y., Kong, X., Spötl, C. and Wang, X., 2013. Improvements in ^{230}Th dating, ^{230}Th and ^{234}U half-life values, and U–Th isotopic measurements by multi-collector inductively coupled plasma mass spectrometry. *Earth and Planetary Science Letters*, *371*, pp.82-91.

Gardner, W.D., Southard, J.B. and Hollister, C.D., 1985. Sedimentation, resuspension and chemistry of particles in the northwest Atlantic. Marine Geology, 65(3-4), pp.199-242.

Hayes, C.T., Anderson, R.F., Fleisher, M.Q., Huang, K.F., Robinson, L.F., Lu, Y., Cheng, H., Edwards, R.L. and Moran, S.B., 2015. ^{230}Th and ^{231}Pa on GEOTRACES GA03, the US GEOTRACES North Atlantic transect, and implications for modern and paleoceanographic chemical fluxes. *Deep Sea Research Part II: Topical Studies in Oceanography*, *116*, pp.29-41.

Honeyman, B.D., Balistrieri, L.S. and Murray, J.W., 1988. Oceanic trace metal scavenging: the importance of particle concentration. *Deep Sea Research Part A. Oceanographic Research Papers*, *35*(2), pp.227-246.

Jerome, S., Bobin, C., Cassette, P., Dersch, R., Galea, R., Liu, H., Honig, A., Keightley, J., Kossert, K., Liang, J. and Marouli, M., 2020. Half-life determination and comparison of activity standards of ^{231}Pa. *Applied Radiation and Isotopes, 155,* p.108837.

Keigwin, L.D. and Jones, G.A., 1989. Glacial-Holocene stratigraphy, chronology, and paleoceanographic observations on some North Atlantic sediment drifts. *Deep Sea Research Part A. Oceanographic Research Papers*, *36*(6), pp.845-867.

Lerner, P., Marchal, O., Lam, P.J., Buesseler, K. and Charette, M., 2017. Kinetics of thorium and particle cycling along the US GEOTRACES North Atlantic Transect. *Deep Sea Research Part I: Oceanographic Research Papers*, *125*, pp.106-128.

McCave, I.N., 1984. Size spectra and aggregation of suspended particles in the deep ocean. *Deep Sea Research Part A. Oceanographic Research Papers*, *31*(4), pp.329-352.

Rutgers van der Loeff, M.M. and Boudreau, B.P., 1997. The effect of resuspension on chemical exchanges at the sediment-water interface in the deep sea—a modelling and natural radiotracer approach. *Journal of Marine Systems*, *11*(3-4), pp.305-342.

Sarmiento, J.L. and Biscaye, P.E., 1986. Radon 222 in the benthic boundary layer. *Journal of Geophysical Research: Oceans*, *91*(C1), pp.833-844.

Schlitzer, R., Anderson, R.F., Dodas, E.M., Lohan, M., Geibert, W., Tagliabue, A., Bowie, A., Jeandel, C., Maldonado, M.T., Landing, W.M. and Cockwell, D., 2018. The GEOTRACES intermediate data product 2017. *Chemical Geology*, *493*, pp.210-223.

Yu, E.F., Francois, R. and Bacon, M.P., 1996. Similar rates of modern and last-glacial ocean thermohaline circulation inferred from radiochemical data. *Nature*, *379*(6567), p.689.